doi:10.1246/cl.2011.162

Published on the web January 15, 2011

Effect of $TiCl_4$ Treatment on Porous ZnO Photoelectrodes for Dye-sensitized Solar Cells

Nobuya Sakai,[1] Norimichi Kawashima,[1,2] and Takurou N. Murakami*[2]
[1]*Graduate School of Engineering, Toin University of Yokohama, 1614 Kurogane, Aoba-ku, Yokohama, Kanagawa 225-8502*
[2]*Faculty of Biomedical Engineering, Toin University of Yokohama, 1614 Kurogane, Aoba-ku, Yokohama, Kanagawa 225-8502*

(Received November 11, 2010; CL-100946; E-mail: murakami@edu.toin.ac.jp)

In this study, photoelectrodes composed of a porous layer of 100-nm ZnO particles are fabricated for use in dye-sensitized solar cells. The electrodes are immersed in an aqueous $TiCl_4$ solution to coat them with a thin layer of TiO_2 for preparation of ZnO–TiO_2 core–shell electrodes. This simple treatment drastically improves the cell performance, resulting in the highest obtained efficiency of 3.91%. This efficiency is higher than that of 100-nm TiO_2 particle cells.

To date, dye-sensitized solar cells (DSSCs) have been able to achieve 11% solar energy conversion efficiency.[1–3] Although such performance makes DSSCs a viable substitute for amorphous silicon solar cells for use in some electronic devices, it is still necessary to further increase the efficiency of DSSCs so that their use can be scaled to provide energy on the order of gigawatts.[4] For this, technological breakthroughs in terms of better materials are required to advance the development of DSSCs to the next generation. Most photoelectrode technology is based on porous titanium(IV) oxide (TiO_2) semiconductor layers. On the other hand, there are some reports of the application of other metal oxides such as tin(IV) oxide (SnO_2), niobium(V) oxide (Nb_2O_5), and zinc oxide (ZnO) as the main material for photoelectrodes and for covering material on TiO_2 core particles as a core–shell structure.[5,6] In particular, ZnO has a band gap and energy level of the conduction band edge similar to those of TiO_2 and has an electron diffusion coefficient higher than that of TiO_2.[7,8] Furthermore, ZnO crystals can be synthesized and grown in mild conditions, and their morphology can be easily controlled by synthetic conditions. These characteristics make it very suitable for use as the porous semiconductor layer in DSSCs.[9–16] Keis et al. used 150-nm spherical ZnO particles as the semiconductor layer in photoelectrodes and compressed the ZnO layer in order to deposit on the conductive substrate at room temperature.[15] The cells exhibited 5.0% efficiency under 0.1 sun illumination. Moreover, the highest efficiency of 6.58% in ZnO cells was also reported by Saito and Fujihara.[17] These results indicate that ZnO is a promising photoelectrode material. Nevertheless, the performance of ZnO cells is still considerably inferior to that of TiO_2 cells, especially in terms of fill factor (*FF*) and open-circuit voltage (V_{oc}). Carrier recombination in ZnO may be the reason for their inferior performance.[18] In addition, ZnO is chemically unstable and is easily dissolved in acidic and basic solutions. Further, its dye-loading capacity is less than that of TiO_2. One of the possible solutions to these shortcomings is to cover the ZnO with a stable material. Law et al. covered ZnO nanowires with thin layers of TiO_2 and Al_2O_3 by atomic layer deposition (ALD) and obtained a high V_{oc} of over 800 mV.[18] Recently, electrodes composed of aggregated ZnO nanoparticles were also covered by TiO_2 using the same ALD techniques, and the obtained efficiency was 6%. However, V_{oc} and *FF* were still less than 710 mV and 60%, respectively.[19,20] Increasing the V_{oc} and *FF* of ZnO cells can lead to a substantial improvement in their performance. Moreover, although ALD techniques are undoubtedly useful to control the formation of thin metal oxide layers, they require the use of a reactor equipped with a vaccum and evacuation system. It is important to devise a simple method for material deposition to develop a cost-effective photovoltaic cell.

In this study, 100-nm ZnO particles are used as the semiconductor layer in photoelectrodes. The layer is treated by simply immersing a substrate with ZnO layer in an aqueous $TiCl_4$ solution to coat the ZnO with TiO_2 to form a core–shell structure, which will improve the dye adsorption and control the carrier recombination. The performance of cells with these photoelectrodes will be compared to that of 100-nm TiO_2 particle cells.

ZnO and TiO_2 in the form of 100-nm semiconductor powders (Aldrich) were separately dispersed in terpineol (Tokyo Chemical Industry) and ethanol (Kanto Chemical) mixed solvent containing ethyl cellulose (Kanto Chemical) as a binder to prepare viscous semiconductor pastes.[21] The pastes were coated on fluorine-doped tin-oxide-coated glass (FTO-glass, Nippon Sheet Glass), which acts as a transparent conductive oxide substrate, using screen-printing techniques. The substrates were then sintered at 450–500 °C for 30 min to prepare the electrodes with porous semiconductor layer. To fabricate the core–shell electrodes, both the substrates with ZnO layer and with TiO_2 layer were first immersed in a 40 mM aqueous $TiCl_4$ solution at 4 °C for 30 min and were then rinsed with ultrapure water and ethanol. To prepare the counter electrodes, platinum(IV) chloride–isopropanol solutions were cast on FTO-glass substrates, and then the substrates were sintered at 400 °C for 30 min. The ruthenium complex dye, bis(tetrabutylammonium)-[*cis*-di(thiocyanato)bis(2,2′-bipyridyl-4-carboxylate-4′-carboxylic acid)ruthenium(II)], N719 (Aldrich), was used as the photosensitizer and was dissolved in a mixed solvent of acetonitrile and *tert*-butyl alcohol as the same volume for 0.5 mM solution. The electrolyte comprised 0.03 M I_2 (Aldrich), 0.6 M 1-methyl-3-butylimidazolium iodide (Aldrich), 0.1 M guanidinium thiocyanate (Aldrich), and 0.5 M 4-*tert*-butylpyridine (Aldrich) in a mixed solvent of 85% acetonitrile and 15% valeronitrile by volume. The porous semiconductor electrodes were heated to 450 °C for 30 min to clean the semiconductor surface just before immersing them in the dye solution for 24 h to induce dye-sensitization. The photoelectrodes and counter electrodes were arranged according to a face-to-face cell layout. A 25-μm thick film spacer (Surlyn®, Dupont) was inserted between the two electrodes, and the space was filled with the electrolyte. The cell performance was estimated by plotting the photocurrent–voltage relation under simulated solar light (100 mW cm^{-2} with an AM1.5 optical filter, Peccell technologies). The light intensity was confirmed for every measurement using a standard

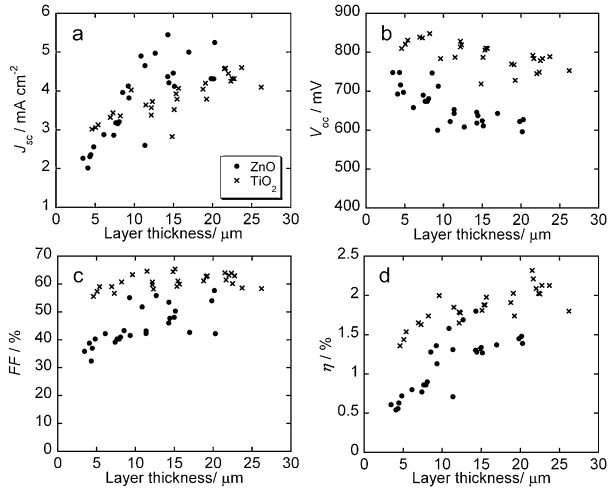

Figure 1. Relation between semiconductor layer thickness in photoelectrode and cell performance in terms of short-circuit current density (J_{sc}, a), open-circuit voltage (V_{oc}, b), fill factor (*FF*, c), and energy conversion efficiency (η, d).

amorphous silicon PV. The surface morphologies and surface elements were observed using scanning electron microscopy and energy-dispersive X-ray spectroscopy (SEM-EDS) (JEOL, JSM-5500LV). Semiconductor layer thickness was measured using laser microscopy (Lasertec, 1LM21DW).

Cell performance is influenced by semiconductor layer thickness. The relation between layer thickness and cell performance is examined for TiO_2 and ZnO cells and is shown in Figure 1. The short-circuit current density (J_{sc}) of both cells increases with an increase in the layer thickness. The ZnO cells exhibit higher current than the TiO_2 cells for layer thicknesses greater than 10 μm. The V_{oc} of both cells decreases with the thickness. The ZnO cells always exhibit lower V_{oc} than the TiO_2 cells regardless of the layer thickness. The *FF* of the ZnO cells is also lower than that of the TiO_2 cells and has significant dependence on the layer thickness. The energy conversion efficiency of both cells increases with the increase in semiconductor layer thickness of up to 14 and 22 μm, respectively. Overall, the efficiency of the TiO_2 cells is higher than that of the ZnO cells.

ZnO and TiO_2 should have conduction band edge of similar energy level. However, the ZnO cells exhibit lower V_{oc} than the TiO_2 cells. In addition, the optimized layer thickness of ZnO is thinner than that of TiO_2. This is probably because of the occurrence of back electron transfer in the ZnO cells, which also causes the voltage loss for thicker ZnO layers. The best performances of the ZnO and TiO_2 cells are 1.80% energy conversion efficiency (J_{sc}, 5.45 mA cm^{-2}; V_{oc}, 618 mV; *FF*, 53.5%) for 14 μm thickness and 2.32% efficiency (J_{sc}, 4.57 mA cm^{-2}; V_{oc}, 792 mV; *FF* 64.0%) for 22 μm thickness, respectively. In these results, the V_{oc} and *FF* of ZnO cells are apparently lower than those of TiO_2, and these should be increased to achieve high performance. For this, the porous ZnO semiconductor electrode was covered with a TiO_2 blocking layer.

The ZnO electrodes with optimum thickness were post-treated by immersing them in an aqueous $TiCl_4$ solution to prepare the ZnO–TiO_2 core–shell electrodes. The morphology of a ZnO–TiO_2 core–shell electrode is compared to that of a ZnO

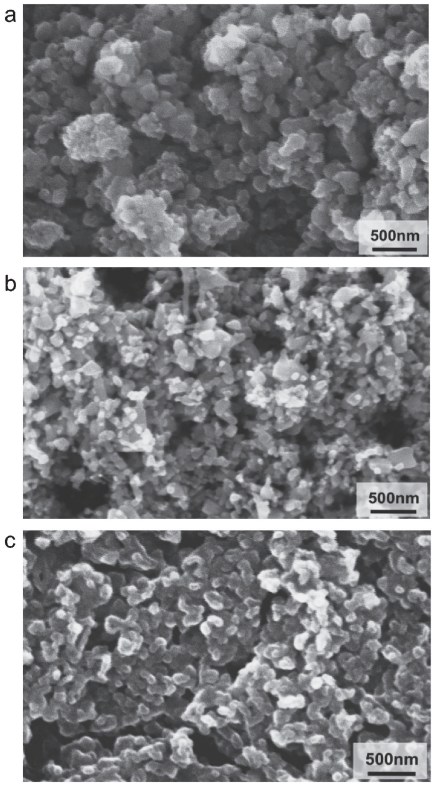

Figure 2. SEM images of TiO_2 (a), ZnO (b), and ZnO–TiO_2 core–shell (c) in the photoelectrodes.

Table 1. Performances of cells having different kinds of semiconductor layers, viz., ZnO, ZnO–TiO_2 core–shell, TiO_2, and TiO_2–TiO_2 core–shell[a]

	Thickness /μm	J_{sc} /mA cm^{-2}	V_{oc}/mV	*FF*/%	η/%
ZnO	14.6 ± 0.40	4.52 ± 0.54	627 ± 14.2	49.1 ± 2.86	1.40 ± 0.23
ZnO–TiO_2 core–shell	12.0 ± 1.45	6.12 ± 0.51	870 ± 33.6	64.4 ± 5.12	3.43 ± 0.31
TiO_2	22.3 ± 0.92	4.51 ± 0.12	778 ± 19.2	62.1 ± 2.13	2.18 ± 0.09
TiO_2–TiO_2 core–shell	22.0 ± 3.02	5.28 ± 0.12	792 ± 13.8	62.0 ± 1.31	2.59 ± 0.08

[a]The layer thickness is determined by noting the thickness range of the best-performing cells, and the data presented is the average of five cells.

electrode. The electrode surfaces are shown in Figure 2. The particles of the core–shell electrode are thicker than those of the ZnO electrode and are almost spherical in shape. The particles in the core–shell electrodes seem to be connected to each other. In the element analysis by EDS, titanium is detected on the particle surface, and it is found that these particles are entirely covered with the elements, titanium and oxygen. The formation of TiO_2 shell during post-treatment may have caused the morphological change in the core–shell electrodes. However, the structured particles fully covering the ZnO core with a thin layer of TiO_2 in a core–shell form have not yet been confirmed, cross-sectional TEM will be carried out in future work to elucidate the ZnO–TiO_2 morphology.

The performances of the cells with optimized semiconductor thickness are listed in Table 1. With the core–shell treatment,

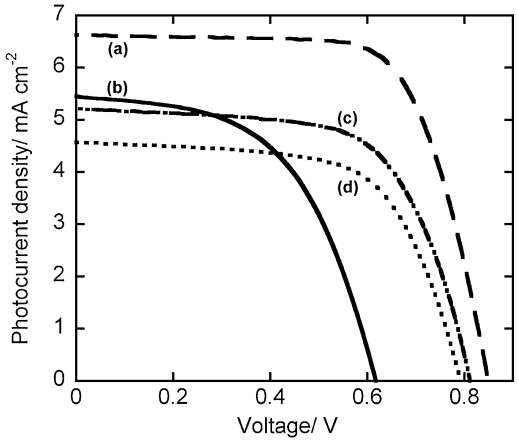

Figure 3. Photocurrent–voltage curves of the best-performance cells for each kind of semiconductor layer, viz., ZnO–TiO_2 core–shell (a), ZnO (b), TiO_2–TiO_2 core–shell (c), and TiO_2 (d).

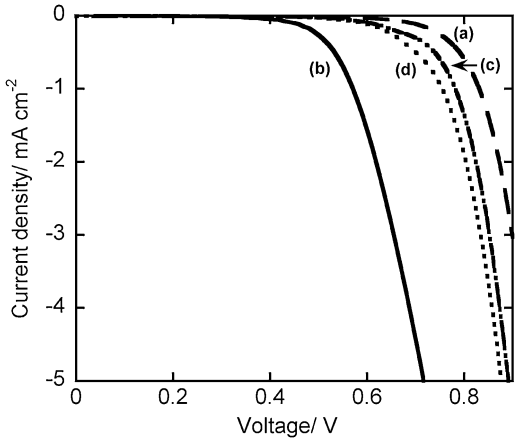

Figure 4. Current–voltage curves of the best-performance cells for each kind of semiconductor layer, viz., ZnO–TiO_2 core–shell (a), ZnO (b), the TiO_2–TiO_2 core–shell (c), and TiO_2 (d) when they are kept in the dark.

the V_{oc} and J_{sc} of both the TiO_2 and the ZnO cells increases. In particular, the ZnO cell exhibits a drastic improvement in performance. The ZnO–TiO_2 core–shell cell exhibits the highest J_{sc} of 6.12 mA cm^{-2}, V_{oc} of 870 mV, *FF* of 64.4%, and efficiency of 3.43%. Although the standard ZnO cell exhibits lower efficiency than the TiO_2 cell, the average efficiency of the ZnO cell increases by more than a factor of two, achieving the best performance. On the other hand, the performance of the TiO_2 cells is low. This may be because of the composition of the rutile crystal of TiO_2; the composition may include a higher concentration of 100-nm particles than of the common 20-nm particles, leading to the crystal adsorbing a smaller amount of the dye.[22]

Figures 3 and 4 show the photocurrent–voltage curves of the best-performance cells for each kind of semiconductor layer and the curves for the same cells when kept in the dark, respectively. The highest efficiency of 3.91% (J_{sc}, 6.62 mA cm^{-2}; V_{oc}, 849 mV; *FF*, 69.5%) is exhibited by the ZnO–TiO_2 core–shell electrode. The ZnO cell has the highest dark current, whereas the ZnO–TiO_2 core–shell cell suppresses the dark current and shows the lowest dark current. Previous reports have proposed that the core–shell blocks the back electron transfer from semiconductor to electrolyte and from conductive substrate to electrolyte.[18] Hence, the higher dark current in ZnO electrodes may be due to the large back electron transfer from ZnO to electrolyte, whereas in ZnO–TiO_2 core–shell electrodes, the TiO_2 shell on the ZnO possibly suppresses the back electron transfer.

In conclusion, we have shown that the simple process of post-treating ZnO photoelectrode by immersing it in an aqueous $TiCl_4$ solution is very effective in improving its J_{sc}, V_{oc}, and *FF*. In particular, the ZnO–TiO_2 core–shell cell exhibits a drastic increase in V_{oc} of over 35% to 849 mV and that in *FF* of over 69%. Research on the effects of factors such as the control of the electron recombination at the semiconductor electrolyte interface is currently in progress, and we intend to discuss it in future reports.

We wish to thank Nippon Sheet Glass for the kind donation of the FTO-glass. This work was partly supported by Strategic International Cooperative Program, Japan Science and Technology Agency (JST).

References

1 M. K. Nazeeruddin, F. De Angelis, S. Fantacci, A. Selloni, G. Viscardi, P. Liska, S. Ito, T. Bessho, M. Grätzel, *J. Am. Chem. Soc.* **2005**, *127*, 16835.
2 Y. Chiba, A. Islam, Y. Watanabe, R. Komiya, N. Koide, L. Han, *Jpn. J. Appl. Phys.* **2006**, *45*, L638.
3 T. Bessho, S. M. Zakeeruddin, C.-Y. Yeh, E. W.-G. Diau, M. Grätzel, *Angew. Chem., Int. Ed.* **2010**, *49*, 6646.
4 M. Grätzel, *Chem. Lett.* **2005**, *34*, 8.
5 Z. Wang, C. Huang, Y. Huang, Y. Hou, P. Xie, B. Zhang, H. Cheng, *Chem. Mater.* **2001**, *13*, 678.
6 A. Kay, M. Grätzel, *Chem. Mater.* **2002**, *14*, 2930.
7 A. J. Nozik, R. Memming, *J. Phys. Chem.* **1996**, *100*, 13061.
8 G. Marcì, V. Augugliaro, M. J. López-Muñoz, C. Martín, L. Palmisano, V. Rives, M. Schiavello, R. J. D. Tilley, A. M. Venezia, *J. Phys. Chem. B* **2001**, *105*, 1033.
9 H. Tsubomura, M. Matsumura, Y. Nomura, T. Amamiya, *Nature* **1976**, *261*, 402.
10 H. Rensmo, K. Keis, H. Lindström, S. Södergren, A. Solbrand, A. Hagfeldt, S.-E. Lindquist, L. N. Wang, M. Muhammed, *J. Phys. Chem. B* **1997**, *101*, 2598.
11 T. Yoshida, H. Minoura, *Adv. Mater.* **2000**, *12*, 1219.
12 T. Yoshida, M. Iwaya, H. Ando, T. Oekermann, K. Nonomura, D. Schlettwein, D. Wöhrle, H. Minoura, *Chem. Commun.* **2004**, 400.
13 M. Law, L. E. Greene, J. C. Johnson, R. Saykally, P. Yang, *Nat. Mater.* **2005**, *4*, 455.
14 K. Keis, J. Lindgren, S.-E. Lindquist, A. Hagfeldt, *Langmuir* **2000**, *16*, 4688.
15 K. Keis, C. Bauer, G. Boschloo, A. Hagfeldt, K. Westermark, H. Rensmo, H. Siegbahn, *J. Photochem. Photobiol., A* **2002**, *148*, 57.
16 Q. Zhang, C. S. Dandeneau, X. Zhou, G. Cao, *Adv. Mater.* **2009**, *21*, 4087.
17 M. Saito, S. Fujihara, *Energy Environ. Sci.* **2008**, *1*, 280.
18 M. Law, L. E. Greene, A. Radenovic, T. Kuykendall, J. Liphardt, P. Yang, *J. Phys. Chem. B* **2006**, *110*, 22652.
19 H. Cheng, W. Hsieh, *Energy Environ. Sci.* **2010**, *3*, 442.
20 K. Park, Q. Zhang, B. B. Garcia, X. Zhou, Y. Jeong, G. Cao, *Adv. Mater.* **2010**, *22*, 2329.
21 S. Ito, P. Chen, P. Comte, M. K. Nazeeruddin, P. Liska, P. Pechy, M. Grätzel, *Prog. Photovoltaics* **2007**, *15*, 603.
22 N.-G. Park, J. van de Lagemaat, A. J. Frank, *J. Phys. Chem. B* **2000**, *104*, 8989.

